

# Fully Automated Lung Volume Assessment from MRI in a Population-based Child Cohort Study

Tatyana Ivanovska<sup>1</sup>, Pierluigi Ciet<sup>2</sup>, Adria Rerez-Rovira<sup>2</sup>, Anh Nguyen<sup>2</sup>, Harm Tiddens<sup>2</sup>, Liesbeth Duijts<sup>2</sup>, Marleen de Bruijne<sup>2</sup> and Florentin Wörgötter<sup>1</sup>

<sup>1</sup>*Department for Computational Neuroscience, Georg-August-University, Göttingen, Germany*

<sup>2</sup>*Erasmus MC: University Medical Center Rotterdam, Rotterdam, Netherlands*

**Keywords:** MRI, Lung, Segmentation and Volumetry, Child Cohort.

**Abstract:** In this work, a framework for fully automated lung extraction from magnetic resonance imaging (MRI) inspiratory data that have been acquired within a on-going epidemiological child cohort study is presented. The method's main steps are intensity inhomogeneity correction, denoising, clustering, airway extraction and lung region refinement. The presented approach produces highly accurate results (Dice coefficients  $\geq 95\%$ ), when compared to semi-automatically obtained masks, and has potential to be applied to the whole study data.

## 1 INTRODUCTION

Magnetic resonance imaging (MRI) is a non-invasive, non-ionizing 3D imaging method that is increasingly applied in research settings. Numerous MR data are acquired from thousands of subjects (Völzke et al., 2011; Hetterich et al., 2015).

Thereafter, the parameters of interest, such as lung or liver volumes, need to be extracted from the images. Manual processing is rather unfeasible due to time constraints and inter- and intra-observer variability. Therefore, automated methods for segmentation of different organs from MRI are developed (Balafar et al., 2010; Setarehdan and Singh, 2012; Ivanovska et al., 2014; Toennies et al., 2015).

However, in a child cohort MR technique is not so easily implementable, since the participants might be scared of the closed environment or the necessity to lie still for some amount of time. Moreover, children anatomy varies widely due to the different stages of growth. Thus, anatomical assumptions used to develop algorithms for adult data might not hold, and, therefore, the methods implemented for adult subjects may not be directly applicable.

Here, we discuss the data from a population-based prospective study with a child cohort and, in particular, a lung segmentation problem from these data, and propose a fully automated solution for lung segmentation.

The paper is organized as follows. In Section 3, the general study information as well as MR protocols

are presented. The ultimate goals of the pulmonary study and the structured step-by-step tasks are formulated in Section 4.1. In Section 2, related works are discussed. The algorithmic solution is proposed in Section 4.2. The results and findings are presented and discussed in Section 5. The Section 6 concludes the paper.

## 2 RELATED WORK

In recent years, multiple automated approaches for lung segmentation were proposed (Ivanovska et al., 2016; Ivanovska et al., 2012; Tustison et al., 2015; Kohlmann et al., 2015; Heimann et al., 2012) have been proposed. The approaches for detection of the lung volumes from anatomical MR scans can be roughly separated in two groups: classical intensity-based and model-based methods. The model-based methods consist from a prior model or atlas construction (Tustison et al., 2015; Tustison et al., 2011), and require usually a significant amount of training data.

The intensity-based methods (Ivanovska et al., 2012; Kohlmann et al., 2015) rely on some low-level features and general considerations on human lung anatomy. Such methods are usually fast and require no prior training.

Although there are some methods for airway system segmentation available, there are only few methods that have been proposed for analysis of child airway MR data. Heimann et al. (Heimann et al.,

2012) presented a method for automated scoring of regional lung perfusion in children with cystic fibrosis using contrast enhanced MRI. They used a combined intensity- and model-based approach. Arens et al. (Arens et al., 2003) applied a fuzzy connectedness approach to perform a detailed analysis of the upper airway (Liu et al., 2002) in children with obstructive sleep apnea. Thayyil et al. (Thayyil et al., 2009) used a semiautomatic method for non-invasive internal organ weight measurement using post-mortem MR imaging in fetuses, newborns, and children.

### 3 MATERIALS

#### 3.1 Information on the Generation R Study

The Generation R Study is a population-based prospective cohort study, which is initiated in Rotterdam, the Netherlands, from fetal life until adulthood. The study is designed to identify the early environmental and genetic causes and causal pathways leading to normal and abnormal growth, development and health during fetal life, childhood and adulthood. The study focuses on six areas of research:

- maternal health;
- growth and physical development;
- behavioral and cognitive development;
- respiratory health and allergies;
- diseases in childhood;
- health and healthcare for children and their parents.

Main exposures of interest include environmental, endocrine, genetic and epigenetic, lifestyle related, nutritional and socio-demographic determinants. In total, 9778 mothers with a delivery date from April 2002 until January 2006 were enrolled in the study. Response at baseline was 61 %, and general follow-up rates until the age of 6 years exceed 80 %. Data collection in mothers, fathers and children include questionnaires, detailed physical and ultrasound examinations, behavioral observations, and biological samples. A genome and epigenome wide association screen is available in the participating children. From the age of 5 years, regular detailed hands-on assessments are performed in a dedicated research center including advanced imaging facilities such as Magnetic Resonance Imaging (MRI). Eventually, results forthcoming from the Generation R Study contribute to the development of strategies for optimizing health (Jaddoe et al., 2012).

#### 3.2 MRI Protocol

The goal of the MRI-study, which comprises approximately 4000 children aged 9, is to assess cardiac, pulmonary, fat, and liver parameters. The MR scanner is a 3-T MR 750w (GE Healthcare, Milwaukee, WI, USA). The pulmonary sequence is the 3D Spoiled Gradient Echo (SPGR) at end-inspiration and end-expiration repeated twice (2 insp and 2 exp). The parameters are: TR=repitition time: 1.6 ms, TE=echo time: 0.7 ms, Flip angle=2°; Average: 0.75, FOV=40cm; Matrix= 200 × 200, in-plane resolution 2 × 2 × 2 mm<sup>3</sup>, 32 channel torso coil. Additionally, a mock scanner is used, in which children can practice to lie within the MR scanner in a friendly way and get used to the scanner protocols.

#### 3.3 Test Set and Expert Annotations

To evaluate the approach, we randomly selected ten subjects and evaluated two inspiratory scans for each of them, i.e., twenty datasets were used as a test set.

We asked an experienced observer to semi-automatically measure lung volumes including trachea with a simple global thresholding, which was a reasonable trade-off between the time and measurement accuracy.

It has to be noted that with such an approach trachea was included in the lung volume, whereas the automated method produces the results without the tracheal volume. This does not appear to be a problem though, due to the fact that trachea is a relatively small organ, when compared to lungs, and its volume is a minor addition (about 200-300 ml) to the total lung volume. Moreover, the spirometry parameters do not exclude the tracheal volume as well. However, in the automatic approach, the trachea is detected and excluded, since we are interested in separate lung volumes as well as further tracheal analysis is planned for future work.

The expert evaluated each dataset two times. In Section 5, two rounds of measurements are denoted as  $R_{e1}$  and  $R_{e2}$ .

## 4 METHODS

### 4.1 Formulated Task

The ultimate goal of the research is to fully analyze the pulmonary system in a child cohort study using the available MRI data. The sub-tasks include (but are not limited to)

1. assessment of lung volumes from inspiratory MR scans;
2. their correlation with spirometry data;
3. analysis of tracheal dimensions;
4. analysis of expiratory lung data.

In this work, we propose a solution to the first sub-task, namely, a fully automated framework for lung volume extraction in inspiratory MR scans.

## 4.2 Proposed Approach

The proposed algorithm is the extended version of the framework proposed by Ivanovska et al. (Ivanovska et al., 2012). The framework scheme is shown in Figure 1.

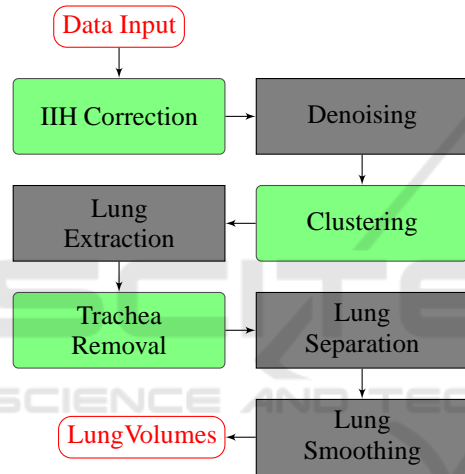


Figure 1: The framework scheme. The modules that differ from the work of Ivanovska et al. (Ivanovska et al., 2012) are marked green.

First, since the study data contain significant intensity inhomogeneity, it requires correction. The recently proposed method N4ITK (Tustison et al., 2010) is applied three times in a row, and the results are of acceptable quality. The example result is shown in Figure 2.

Second, the corrected data are denoised using a boundary preserving method, the classical Anisotropic diffusion filter (Perona et al., 1994), and the intensity clustering, namely, the Fuzzy C-Means (Bezdek et al., 1984) method, is applied.

Third, the regions that are classified to the darkest intensity class are selected, and the background is removed from further processing. Here, a special region evaluation procedure is introduced to prevent the extraction of non-lung regions. We apply a region growing-based procedure, which evaluates the lung region overlap in consecutive slices. Since a

rather smooth lung area decay is expected, any regions that have an overlap with regions in the previous slice smaller than a pre-selected threshold value are disregarded from the further processing.

Fourth, the tracheal, namely, dark tubular regions are identified using the Vesselness filter (Frangi et al., 1998). It analyzes the eigenvalues of the Hessian matrix. Thereafter, the filter’s response is overlaid with the lung mask segmented in the previous step. Then, the tracheal region is tracked and the cut is made, where main bronchi enter the lung parenchyma. The Vesselness filter allows one to detect tracheal regions even in the cases, where there is no clearly visible boundary between the trachea and the lung tissue.

Finally, the lung regions are separated with pre-filled 3D Watershed (Roerdink and Meijster, 2000) and smoothed with morphological operations (Sonka et al., 2014) similar to the approach of Ivanovska et al. (Ivanovska et al., 2011). The lung masks and volumes are computed and saved to a file.

In Figure 3, we present 3D and 2D example results, demonstrating the excluded trachea and smoothed lungs.

## 5 RESULTS AND DISCUSSION

The automated approach was implemented in the MeVisLab Framework (Heckel et al., 2009). The parameters were fixed for the test set. Average computation time for each dataset is about 3-4 minutes on a AMD Athlon II X4 860K, 4x 3700 MHz with 16 GB DDR3-RAM.

To evaluate the expert readings and automatically computed results, we use two metrics, namely, the DICE coefficient (Dice, 1945) and the Jaccard index (Real and Vargas, 1996). The definition of the metrics is given below. For two sets, in our case, the results obtained from the expert and the automatically computed results,  $R_e$  and  $R_a$ , respectively, the overlap coefficients are computed as

$$DSC = \frac{2|R_e \cap R_a|}{|R_e| + |R_a|} \quad (1)$$

$$Jacc = \frac{|R_e \cap R_a|}{|R_e \cup R_a|} \quad (2)$$

Since our observer analyzed the test set two times, we assess the intra-observer variability and compare the automatically obtained results  $R_a$  to both expert measurements, denoted  $R_{e1}$  and  $R_{e2}$ , respectively. The comparison results (mean  $\mu \pm$  standard deviation  $\sigma$ ) for 20 test datasets are presented in Table 1. We evaluated the intra-observer variability using the same

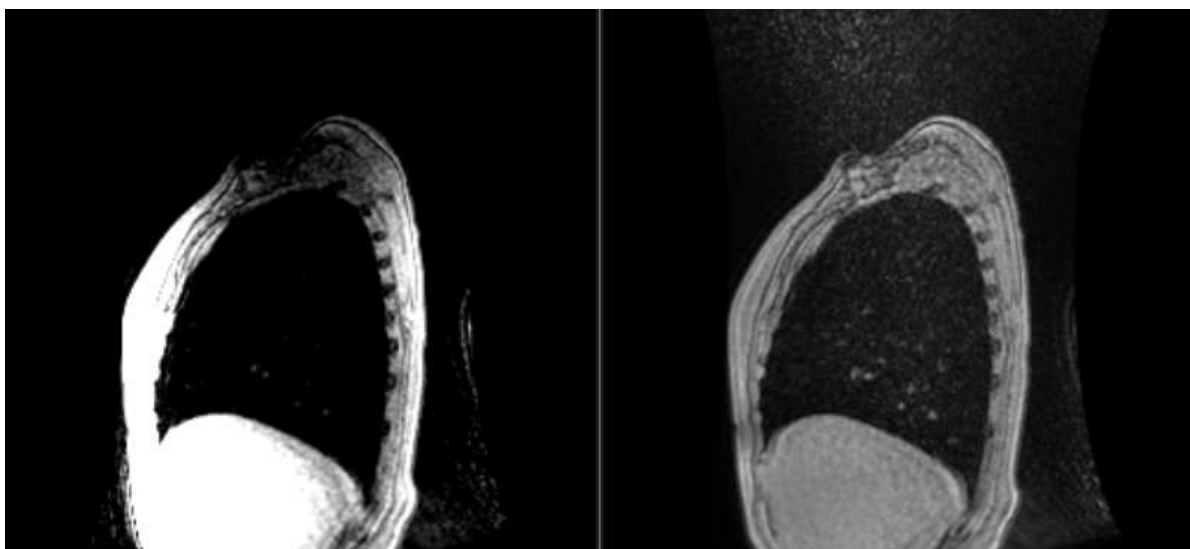


Figure 2: Example slice in a sagittal view. Left: original data; Right: corrected data with three consecutive N4ITK cycles.

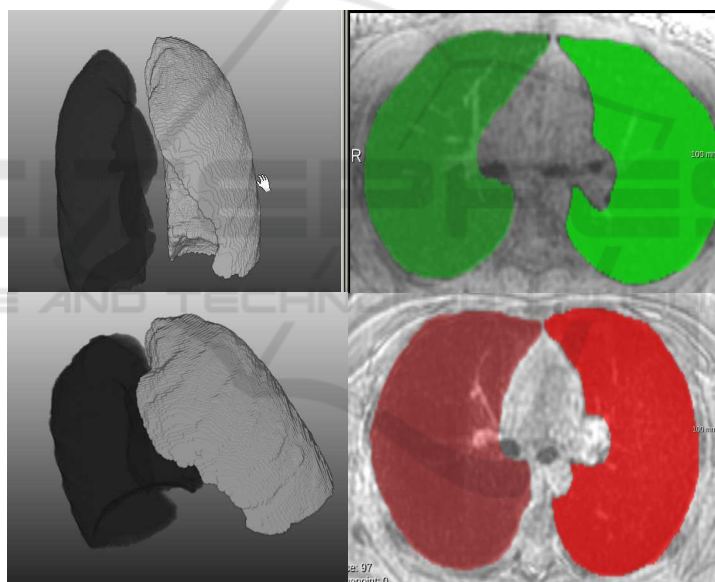


Figure 3: Example results from 2 datasets. Left: 3D results; Right: Segmentation results are overlaid with the original data in axial projection.

metrics, and for  $R_{e1}$  vs  $R_{e2}$  the DICE and Jaccard coefficients are  $0.9674 \pm 0.00597$  and  $0.9364 \pm 0.02$ , respectively.

As one can observe, the automatically computed results lie close to both semi-automatically obtained ground truth masks, and the Dice coefficient is about 95%. The differences are due to the fact that the expert neither excluded the tracheal region from the evaluation nor smoothed the lung regions. In Figure 4, an overlay example of the expert readings (white) and the automated results (green) are documented. The

Table 1: Manual and automated result comparison.

Proposed approach		Previous method (Ivanovska et al., 2011)	
DICE	Jaccard	DICE	Jaccard
$R_a$ vs. $R_{e1}$		$R_a$ vs. $R_{e1}$	
$0.9521 \pm 0.010$	$0.9083 \pm 0.01$	$0.8901 \pm 0.11$	$0.82 \pm 0.0968$
$R_a$ vs. $R_{e2}$		$R_a$ vs. $R_{e2}$	
$0.95485 \pm 0.018$	$0.9145 \pm 0.01$	$0.8875 \pm 0.0906$	$0.81 \pm 0.1004$

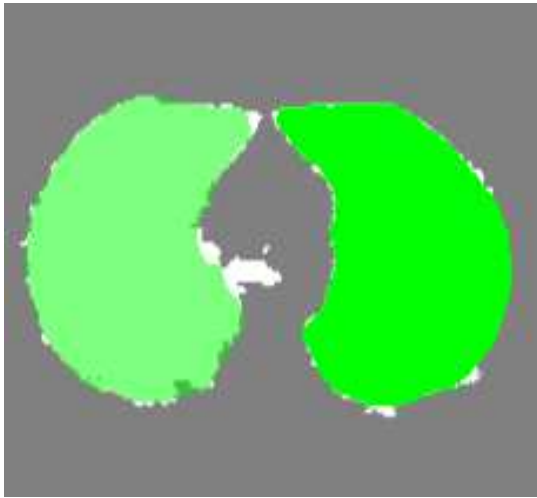


Figure 4: Comparison of manual readings (white) and automated results (green) in 2D.

expert readings differ from each other slightly (the Dice coefficient is about 97%), since the differences are only due to the selected global threshold value.

Additionally, we applied the technique of Ivanovska et al. (Ivanovska et al., 2011) to our test set. That method was designed for and tested on a different sequence with a higher spatial resolution and less artifacts. The results are also presented in Table 1. The previous technique did not include any intensity inhomogeneity correction and the trachea removal procedure was based only on region growing in the segmentation mask. We assume that this affected the results negatively (the DICE coefficient is less than 90%), since in some cases the parts of lungs were either oversegmented or undersegmented and misinterpreted as other structures and erroneously removed. The proposed pipeline successfully overcomes these problems and produces accurate results.

## 6 CONCLUSIONS AND FUTURE WORK

In this paper, a fully automated approach for lung segmentation in MRI data from the Generation R child study. The results were applied to a sample of 20 datasets. Our expert established groundtruth in a semi-automatic manner in two measurement sessions. We assessed the segmentation accuracy by comparing the automatically computed results to the expert readings. Moreover, the comparison to a previously established technique was also done. The proposed framework produces highly accurate results and has a potential to be applied to the whole pulmonary dataset

(above 4000 subjects).

Future extensions of the framework include analysis of tracheal regions and segmentation of expiratory scans.

## REFERENCES

- Arens, R., McDonough, J. M., Corbin, A. M., Rubin, N. K., Carroll, M. E., Pack, A. I., Liu, J., and Udupa, J. K. (2003). Upper airway size analysis by magnetic resonance imaging of children with obstructive sleep apnea syndrome. *American journal of respiratory and critical care medicine*, 167(1):65–70.
- Balafar, M. A., Ramli, A. R., Saripan, M. I., and Mashohor, S. (2010). Review of brain mri image segmentation methods. *Artificial Intelligence Review*, 33(3):261–274.
- Bezdek, J. C., Ehrlich, R., and Full, W. (1984). Fcm: The fuzzy c-means clustering algorithm. *Computers & Geosciences*, 10(2):191–203.
- Dice, L. R. (1945). Measures of the amount of ecologic association between species. *Ecology*, 26(3):297–302.
- Frangi, A. F., Niessen, W. J., Vincken, K. L., and Viergever, M. A. (1998). Multiscale vessel enhancement filtering. In *Medical Image Computing and Computer-Assisted Intervention MICCAI98*, pages 130–137. Springer.
- Heckel, F., Schwier, M., and Peitgen, H.-O. (2009). Object-oriented application development with mevislab and python. In *GI Jahrestagung*, pages 1338–1351. Cite-seer.
- Heimann, T., Eichinger, M., Bauman, G., Bischoff, A., Puderbach, M., and Meinzer, H.-P. (2012). Automated scoring of regional lung perfusion in children from contrast enhanced 3d mri. In *SPIE Medical Imaging*, pages 83150U–83150U. International Society for Optics and Photonics.
- Hetterich, H., Bayerl, C., Peters, A., Heier, M., Linkohr, B., Meisinger, C., Auweter, S., Kannengießer, S. A., Kramer, H., Ertl-Wagner, B., et al. (2015). Feasibility of a three-step magnetic resonance imaging approach for the assessment of hepatic steatosis in an asymptomatic study population. *European radiology*, pages 1–10.
- Ivanovska, T., Buttke, E., Laqua, R., Völzke, H., and Beule, A. (2011). Automatic trachea segmentation and evaluation from mri data using intensity pre-clustering and graph cuts. In *Image and Signal Processing and Analysis (ISPA), 2011 7th International Symposium on*, pages 513–518. IEEE.
- Ivanovska, T., Hegenscheid, K., Laqua, R., Gläser, S., Ewert, R., and Völzke, H. (2016). Lung segmentation of mr images: A review. In *Visualization in Medicine and Life Sciences III*, pages 3–24. Springer.
- Ivanovska, T., Hegenscheid, K., Laqua, R., Kühn, J.-P., Gläser, S., Ewert, R., Hosten, N., Puls, R., and Völzke, H. (2012). A fast and accurate automatic lung segmentation and volumetry method for mr data used in epidemiological studies. *Computerized Medical Imaging and Graphics*, 36(4):281–293.

- Ivanovska, T., Laqua, R., Wang, L., Liebscher, V., Völzke, H., and Hegenscheid, K. (2014). A level set based framework for quantitative evaluation of breast tissue density from mri data. *PLoS one*, 9(11):e112709.
- Jaddoe, V. W., van Duijn, C. M., Franco, O. H., van der Heijden, A. J., van Ilzendoorn, M. H., de Jongste, J. C., van der Lugt, A., Mackenbach, J. P., Moll, H. A., Raat, H., et al. (2012). The generation r study: design and cohort update 2012. *European journal of epidemiology*, 27(9):739–756.
- Kohlmann, P., Strehlow, J., Jobst, B., Krass, S., Kuhnigk, J.-M., Anjorin, A., Sedlaczek, O., Ley, S., Kauczor, H.-U., and Wielpütz, M. O. (2015). Automatic lung segmentation method for mri-based lung perfusion studies of patients with chronic obstructive pulmonary disease. *International journal of computer assisted radiology and surgery*, 10(4):403–417.
- Liu, J., Udupa, J. K., Odhner, D., McDonough, J. M., and Arens, R. (2002). Upper airway segmentation and measurement in mri using fuzzy connectedness. In *Medical Imaging 2002*, pages 238–247. International Society for Optics and Photonics.
- Perona, P., Shiota, T., and Malik, J. (1994). Anisotropic diffusion. In *Geometry-driven diffusion in computer vision*, pages 73–92. Springer.
- Real, R. and Vargas, J. M. (1996). The probabilistic basis of jaccard's index of similarity. *Systematic biology*, 45(3):380–385.
- Roerdink, J. B. and Meijster, A. (2000). The watershed transform: Definitions, algorithms and parallelization strategies. *Fundamenta informaticae*, 41(1, 2):187–228.
- Setarehdan, S. K. and Singh, S. (2012). *Advanced algorithmic approaches to medical image segmentation: state-of-the-art applications in cardiology, neurology, mammography and pathology*. Springer Science & Business Media.
- Sonka, M., Hlavac, V., and Boyle, R. (2014). *Image processing, analysis, and machine vision*. Cengage Learning.
- Thayyil, S., Schievano, S., Robertson, N. J., Jones, R., Chitty, L. S., Sebire, N. J., Taylor, A. M., group, M. M. R. I. A. S. C., et al. (2009). A semi-automated method for non-invasive internal organ weight estimation by post-mortem magnetic resonance imaging in fetuses, newborns and children. *European journal of radiology*, 72(2):321–326.
- Toennies, K. D., Gloger, O., Rak, M., Winkler, C., Klemm, P., Preim, B., and Völzke, H. (2015). Image analysis in epidemiological applications. *it-Information Technology*, 57(1):22–29.
- Tustison, N. J., Avants, B. B., Cook, P. A., Zheng, Y., Egan, A., Yushkevich, P. A., and Gee, J. C. (2010). N4itk: improved n3 bias correction. *Medical Imaging, IEEE Transactions on*, 29(6):1310–1320.
- Tustison, N. J., Avants, B. B., Flors, L., Altes, T. A., de Lange, E. E., Mugler, J. P., and Gee, J. C. (2011). Ventilation-based segmentation of the lungs using hyperpolarized <sup>3</sup>he mri. *Journal of Magnetic Resonance Imaging*, 34(4):831–841.
- Tustison, N. J., Qing, K., Wang, C., Altes, T. A., and Mugler, J. P. (2015). Atlas-based estimation of lung and lobar anatomy in proton mri. *Magnetic resonance in medicine*.
- Völzke, H., Alte, D., Schmidt, C. O., Radke, D., Lorbeer, R., Friedrich, N., Aumann, N., Lau, K., Piontek, M., Born, G., et al. (2011). Cohort profile: the study of health in pomerania. *International journal of epidemiology*, 40(2):294–307.